Annual CO_2 and CH_4 fluxes in coastal earthen ponds with *Litopenaeus vannamei* in southeastern China

Chuan Tong[a,b], David Bastviken[c], Kam W. Tang[d], Ping Yang[a,b‡], Hong Yang[e,f,g‡], Yifei Zhang[b], Qianqian Guo[b], Derrick Y. F. Lai[h,‡]

[a]*Key Laboratory of Humid Subtropical Eco-geographical Process of Ministry of Education, Fujian Normal University, Fuzhou 350007, P.R. China*

[b]*School of Geographical Sciences, Fujian Normal University, Fuzhou 350007, P.R. China*

[c]*Department of Thematic Studies–Environmental Change, Linköping University, Linköping, Sweden*

[d]*Department of Biosciences, Swansea University, Swansea SA2 8PP, U. K.*

[e]*Collaborative Innovation Center of Atmospheric Environment and Equipment Technology, Jiangsu Key Laboratory of Atmospheric Environment Monitoring and Pollution Control (AEMPC), School of Environmental Science and Engineering, Nanjing University of Information Science & Technology, 219 Ningliu Road, Nanjing 210044, China*

[f]*College of Environmental Science and Engineering, Fujian Normal University, Fuzhou, 350007, China*

[g]*Department of Geography and Environmental Science, University of Reading, Reading, UK*

[h]*Department of Geography and Resource Management, The Chinese University of Hong Kong, Shatin, New Territories, Hong Kong SAR, China*

[‡]**Correspondence to:**

P. Yang (yangping528@sina.cn, Telephone 086-0591-87445659) or H. Yang (hongyanghy@gmail.com, Telephone 0044(0)1183787750) or Derrick Y.F. Lai (dyflai@cuhk.edu.hk, Telephone 852-39436528)

A B S T R A C T

Small-scale aquaculture operation is increasing rapidly in the world, particularly in developing countries, but the greenhouse gas (GHG) dynamics and fluxes from small aquaculture ponds are still poorly assessed. In this study, dissolved concentrations and fluxes of CO_2 and CH_4 were determined in three coastal earthen shrimp ponds over one whole year, including both farming and non-farming periods, in the Min River Estuary, southeastern China. Different from many previous studies, both ebullitive and diffusive CH_4 fluxes were measured. The average concentrations of dissolved CO_2 and CH_4 in water column in the farming period varied between 18.1±0.1 and 79.6±1.1 μmol L^{-1}, and 1.3±0.1 and 55.9±3.2 μmol L^{-1}, respectively. Averaged across the whole year, the mean CO_2 and CH_4 fluxes from the ponds were –18.4±7.4 and 22.6±6.9 mg m^{-2} h^{-1}, respectively, suggesting that the shrimp ponds worked as a CO_2 sink and a CH_4 source. Based on the sustained-flux global warming potential (SGWP) and sustained-flux global cooling potential (SGCP) models, the annual warming potential was estimated to be 7.1×10^3 g CO_2-eq m^{-2} yr^{-1}, with approximately 90% from the farming period. Ebullition was the dominant emission pathway for CH_4, accounting for over 90% of the total CH_4 emission during the farming period. The full-year study improves the understanding of carbon cycling in coastal aquaculture ponds and provides scientific basis for updating GHG inventories.

Keywords: Carbon dioxide; Methane; Annual fluxes; Emission pathway; Coastal aquaculture ponds; Global change

1. Introduction

Carbon dioxide (CO_2) and methane (CH_4) are two very potent greenhouse gases (GHGs). The atmospheric levels of these two GHGs have increased by ca. 44% and 156% since 1750, reaching 414 ppm and 1875 ppb, respectively, in 2019 (National Oceanic and Atmospheric, 2020). Studies have estimated that global inland waters release 2.1 Pg C yr^{-1} of CO_2 (Raymond et al., 2013) and 0.65 Pg C yr^{-1} of CH_4 (Bastviken et al., 2011). Hence, GHG emission from continental aquatic ecosystems plays an important role in the overall carbon cycle and climate forcing (Bastviken et al., 2011; Tranvik et al., 2009).

Small ponds (<0.01 km^2) has been suggested to have the largest GHG emissions per unit area, but data are still rare and emissions from different kinds of pond are far from clear (Holgerson, 2015). Downing (2010) estimated that there can be as many as 3.2 billion very small ponds (< 0.001km^2) with a total surface area of ca. 0.8 million km^2 in the world. These ponds can be hotspots for GHG emissions because of the large loadings of both exogenous and endogenous organic matters to fuel GHG production (Holgerson, 2015; Rubbo et al., 2006). Therefore, detailed assessments of *in situ* concentrations and fluxes of GHGs in small ponds are crucial for improving the global GHG budgets (Holgerson, 2015; Holgerson and Raymond, 2016). Of particular interest are aquaculture ponds, which have large amounts of carbon and nutrient loading (Yuan et al., 2019; Yuan et al., 2021). While some preliminary results point to their importance in national GHG inventories especially in aquaculture-intensive countries (Yang et al., 2018a, *in situ* measurements of GHG

exchange in aquaculture ponds are still quite rare.

Small-scale aquaculture ponds are wide-spread especially in developing countries (FAO, 2017). The combined global surface area of brackish and freshwater aquaculture ponds is ca. 1.1×10^5 km^2 in 2005 (Verdegem and Bosma, 2009). China, the world's largest producer of aquatic products, has the total aquaculture pond area of ca. 3.2×10^4 km^2 in 2018, i.e. almost one third of the estimated global area (Bureau of Fisheries of the Ministry of Agriculture, 2019). These ponds receive large amounts of organic matter through daily supply of feeds and algal production (Chen et al. 2015; Yang et al. 2018a). Due to their unique biological, physical and chemical characteristics (Zha et al., 2006), the dynamics and fluxes of GHGs in aquaculture ponds can be very different from other aquatic habitats.

Several studies have measured CH_4 and CO_2 fluxes and their driving factors in aquaculture systems in China (e.g., Chen et al., 2016; Hu et al., 2016; Wu et al., 2018; Zhang et al., 2020). However, the data are far from sufficient to understand the biogeochemical cycle of GHGs in aquaculture ponds, given the large number and areal coverage of aquaculture ponds. More importantly, previous studies focused on gas emissions during the farming period only, whereas GHG fluxes at the sediment-air interface during the non-farming period is virtually unknown.

CO_2 is primarily emitted from water surfaces through diffusion across the water-air interface (diffusive flux), driven by the concentration gradient and the gas exchange velocity. CH_4 can be emitted by diffusive flux, ebullition (bubble flux) or the combination of both (Bastviken et al., 2004). Although ebullition is widely

92 recognized as an important CH_4 emission pathway in shallow waters (e.g., Bastviken
93 et al., 2004; Deshmukh et al., 2016; Natchimuthu et al., 2014, 2016; Xiao et al., 2017),
94 field measurements of CH_4 ebullition in aquaculture ponds are rare.

95 To address the knowledge gaps outlined above on CO_2 and CH_4 emissions from
96 aquaculture ponds, this study measured the CH_4 and CO_2 fluxes during both farming
97 and non-farming periods in earthen aquaculture ponds in southeastern China. The
98 intensity of earthen pond aquaculture has increased steadily over the last few decades
99 (Wang et al., 2018). Intensive-farming shrimp pond is the most dominant type of
100 earthen ponds in the coastal region of China with an area of 2.4×10^3 km^2 (Bureau of
101 Fisheries of the Ministry of Agriculture, 2019), accounting for ca. 12% of the total
102 global area of shrimp aquaculture ponds. The main aims of the study were to: (1)
103 determine the spatial and temporal variations in dissolved CO_2 and CH_4
104 concentrations in the farming period; (2) determine the magnitude of CO_2 and CH_4
105 fluxes for the whole year including both farming and non-farming periods; (3) assess
106 the dominant CH_4 emission pathway in the farming period.

107 ## 2. Materials and Methods

108 *2.1. Study Area*

109 The three studied shrimp ponds are located at the Shanyutang Wetland
110 (26°00′36″-26°03′42″ N, 119°34′12″-119°40′40″ E), one of the largest wetlands in the
111 Min River Estuary, Fujian, southeastern China (Fig. 1). This area is dominated by the
112 native plants *Cyperus malaccensis* and *Phragmites australis*, and the invasive species
113 *Spartina alterniflora*. It is in the subtropical monsoon climate zone, and the mean

annual temperature and average annual precipitation are ca. 19.6 °C and 1,350 mm, respectively (Tong et al., 2018). The Min River Estuary is affected by the typical semidiurnal tide, and the surface soil is usually submerged for around 7 hours every day (Tong et al., 2018). In the central-eastern part of the wetland, the mosaic vegetated landscape was cleared and converted to aquaculture ponds for the shrimp species *Litopenaeus vannamei* in the last several years (Yang et al., 2017a).

2.2. Shrimp pond and aquacultural management

Considering the optimal water temperature for shrimp growth (*L. vannamei*; 22 - 35 ºC), farming in the area often begins in June and ends in November (Yang et al., 2017b). In traditional earthen pond shrimp farming, accumulated sediments are not removed regularly. In our ponds, the average sediment accumulation rate was 0.79 cm month^{-1}. Between each production cycle, the first steps of preparation included cleaning and reinforcing the pond bank, and draining the pond to dry the sediment. Next, lime was added to the pond (calcium oxide; 0.5 t ha^{-1}). After that, the brackish water from the adjacent estuary was pumped through a filter bag into the pond. The water depth was relative stable (1.1–1.5 m) during the farming period. Approximately 7 days after filling, the water was disinfected with trichloroisocyanuric acid (1.5 mg L^{-1}). A few days later, fertilizer was added (calcium superphosphate; 1.5–2.0 kg per 1000 m^3) for 7 to 10 consecutive days. A few days before stocking, probiotics (Zhengzhou Nongfukang Biotechnology Co., Zhejiang province, China; 200 mL per 1000 m^2) were added, and basic physico-chemical parameters (e.g., pH, salinity, alkalinity, and water colour) were monitored to ensure they were in the appropriate

136 range.

137 The shrimps were fed commercial food pellets containing 42% crude protein
138 (Hangsheng^{TM} and Tianma^{TM}, Fujian, China) twice per day (7:00 am and 4:00 pm).
139 For aeration, 3-5 paddlewheel aerators were operated 4 times every day (7:00
140 am–9:00 am, 12:00 pm–2:00 pm, 6:00 pm–8:00 pm, and 12:00 am–3:00 am). After
141 harvesting in late November, the pond water was discharged. The non-farming period
142 lasts from December to next May. For more details about the shrimp pond system and
143 the operation, please refer to Table S1 and Yang et al. (2017b).

144 *2.3. Collection and analysis of water and sediment samples*

145 In each pond, a foot-bridge extending ~10 m from the bank to the center was used
146 for sampling at three sites: the first site was close to the bank; the second site in the
147 mid-section of the bridge; the third site at the center of the pond. On each sampling
148 day during the farming period, samples were taken between 9:00 am and 11:00 am
149 and ca. 30 min. after the paddlewheels had been turned off. All sampling sites were at
150 least 6-7 m away from the aerator.

151 At each site, water was taken from three depths: the surface layer (10 cm below
152 the water surface), the middle layer (between surface and bottom layer), and the
153 bottom layer (near the sediment surface). Water samples were collected from each
154 depth using a 1.5-L organic glass hydrophores, and 0.2 mL of saturated $HgCl_2$
155 solution was added into 150 mL water sample to stop microbial activities (Hu et al.,
156 2018; Yang et al., 2017b). All samples were stored in a 4 ^{o}C cooler for later laboratory
157 analysis within 4-6 hours.

158 The water samples were analysed for chlorophyll *a* (Chl *a*), total dissolved
159 nitrogen (TDN), total dissolved phosphorus (TDP) and dissolved organic carbon
160 (DOC). For TDN and TDP, a 50 mL aliquot was filtered through a 0.45 μm filter
161 (Biotrans™ nylon membranes) and the filtrate was analysed by a flow injection
162 analyser (Skalar Analytical SAN^{++}, Netherlands). For DOC, another 50 mL aliquot
163 was filtered and the filtrate was analysed by a Total Organic Carbon analyzer
164 (TOC-VCPH/CPN, Shimadzu, Japan). Chl *a* was measured by spectrophotometry
165 (UV-VIS spectrophotometer, Shimadzu UV-2450, Japan) (Yang et al., 2017b).

166 In the non-farming period, surface sediment (0–15 cm) was collected at each site
167 with a cylindrical metal corer (6 cm diameter). Sediment samples were stored in a 4
168 ^{o}C cooler until analysis. In the laboratory, the sediment samples were freeze-dried and
169 ground to fine powder to determine total carbon (TC) and total nitrogen (TN) by an
170 elemental analyzer (Elementar Vario MAX CN, Germany) (Sun et al., 2013).
171 Sediment water content (SWC) was determined based on weight difference after 24
172 hours oven drying (105 ^{o}C) (Zhang et al., 2013).

173 *2.4. Measurement of dissolved gas concentrations*

174 To determine the dissolved CO_2 and CH_4 concentrations in water column in the
175 farming period, 15 sampling campaigns were conducted between June and November,
176 2017. In each campaign and at each site, water samples were collected with a
177 homemade sampler at 10 cm depth intervals and transferred into glass vials without
178 bubbles. All samples were stored in a 4 ^{o}C cooler for later laboratory analysis.

179 Dissolved CO_2 and CH_4 in the water samples were extracted by the headspace

technique: 25-mL of the water was displaced by injecting N_2 gas (>99.9% purity) into the glass vial. The samples were vigorously shaken to attain air-water equilibrium. After waiting for 30 minutes, CO_2 and CH_4 concentrations in the headspace were determined by a gas chromatography (GC-2010, Shimadzu, Kyoto, Japan) with flame ionization detection (FID) after passing through a methanizer. The dissolved CO_2 and CH_4 concentrations were calculated using the volumes of the headspace and water in the vial and the solubility coefficients of the two gases (Wanninkhof, 1992).

2.5. Gas flux measurement

In the farming period, gas samples were collected using the floating chamber technique (Lorke et al., 2015; Natchimuthu et al., 2014, 2016). The floating chambers (an area of 0.1 m^2 and a volume of 5.2 L) were fitted with Styrofoam around the rims for floatation and were covered in reflective aluminum tape to minimise internal heating by sunlight (Natchimuthu et al. 2016, 2017).

In the non-farming period, gas samples were collected using an enclosed static chamber (Olsson et al., 2015; Tong et al., 2018), which included two components: a 30 cm tall plastics bottom collar with a base dimension of 35×35 cm^2, and a 50 cm tall polyvinyl chloride top chamber with a base dimension of 35 × 35 cm^2. The bottom collar was inserted 18 cm into the sediment (Yang et al., 2018c). An electric fan was installed inside the chamber for mixing.

From both types of chambers, four gas samples were collected using 60 mL plastic syringes equipped with three-way stopcocks at 15-min intervals over a period of 45 min. The collected gas was immediately transferred to an airtight gas sampling bag

(Dalian Delin Gas Packing Co., Ltd., China) and transported back to the laboratory for measurement. CO_2 and CH_4 concentrations in the gas samples were determined using a gas chromatograph (GC-2010, Shimadzu, Kyoto, Japan) equipped with a flame ionization detector (FID) within 24 h of sampling. CO_2 and CH_4 fluxes (mg m^{-2} h^{-1}) were estimated via regressions of concentration and time (Yang et al. 2018a).

Measurements by the floating chamber represented the combination of ebullitive and diffusive fluxes (Chuang et al., 2017; Zhu et al., 2016). To tease apart the two types of flux, first, diffusive CH_4 flux was calculated from surface-water gas concentrations and wind-dependent gas exchange velocity (k) according to the transfer coefficient model (Cole and Caraco 1998). More detailed explanation of the calculations can be found in Xiao et al. (2017) and Yang et al. (2019). The proportion of ebullition was then calculated by subtracting the diffusive flux from the total flux measured by the floating chamber (Chuang et al., 2017; Xiao et al., 2017; Yang et al., 2019). Based on monthly measurements of the gas fluxes, the annual cumulative fluxes of CO_2 and CH_4 were calculated using Eq. (1) (Moore et al. 2011; Song et al. 2009):

$$AE = \sum MF_i \times D_i \times 24\text{hr} \qquad (1)$$

where MF_i is the mean CO_2 (or CH_4) flux in the ith month of the year (mg CH_4 m^{-2} h^{-1}), and D_i is the total number of days in the ith month.

2.6. Measurement of environmental variables

The meteorological variables including precipitation, air temperature, air pressure and wind speed were measured at 30 min intervals at a nearby weather station. In

addition, during the farming period, water temperature, pH, electrical conductivity (EC), and dissolved oxygen (DO) were measured *in situ* at three depths (surface, middle and bottom layers). In the non-farming period, sediment temperature was measured at 15 cm depth at all sites. pH and temperature were measured using a portable pH/mV/Temperature meter system (IQ150, IQ Scientific Instruments, U.S.A.), the EC was measured using a 2265FS EC Meter (Spectrum Technologies, U.S.A.) and DO was measured using a multiparameter probe (550A YSI, USA).

2.7. Statistical analysis

Two–way ANOVA was conducted to examine the effects of sampling depths, sampling time, and their interactions on dissolved CO_2 (or dissolved CH_4) concentrations in the ponds during the farming period. The independent-sample *t*-test was performed to examine the differences in the CO_2 and CH_4 fluxes between the farming and the non-farming periods. Pearson correlation coefficients were used to test the relationships between the CO_2 or CH_4 concentrations (or fluxes) and environmental factors. Stepwise regression analysis was conducted to identify environmental variables that influenced gas fluxes in the farming period. Statistical analyses were performed in SPSS 22.0 (IBM, Armonk, NY, USA) and the results were considered significant at the level of $p < 0.05$.

3. Results

3.1. Physical and chemical properties of water and sediment

During the farming period, physical and chemical properties of the pond water varied significantly between farming time ($p<0.01$), but insignificantly between

246 depths (except for DO) (p>0.05). During the non-farming period, the sediment
247 temperature followed air temperature, with mean value ranging between 10.5°C and
248 28.1°C (Fig. 2a). During the non-farming period, the average sediment TN was
249 2.41±0.11 g kg^{-1} (range 14.8-23.8 g kg^{-1}; Fig. 2b), the average TC was 18.15±0.96 g
250 kg^{-1} (range 1.9-3.1 g kg^{-1}; Fig. 2c) and the average SWC was 34.17±2.56% (range
251 25.4-46.2 %; Fig. 2d). TC, TN and SWC decreased gradually with time.

252 *3.2. Dissolved CO_2 and CH_4 concentrations in water*

253 During the farming period, the average CO_2 concentration at the different depths
254 varied between 18.1 and 79.6 µmol L^{-1} (Fig. 3), with the corresponding saturation rate
255 between 77.4 and 505.5%. There were no significant differences between depths.
256 Across all sampling dates, 53% of the samples were 1.1- to 3.0-fold oversaturated and
257 27% of the samples were > 3.0-fold oversaturated. Average CO_2 concentration was
258 substantially higher at all depths in mid-August to early September than in the other
259 months (F=3.480, p<0.01, two-ANOVA; Fig. 3).

260 The average CH_4 concentration at the different depths in the farming period varied
261 between 1.3±0.9 and 55.9±32.7 µmol L^{-1} (Fig. 4). CH_4 concentration varied
262 significantly between sampling periods (F=12.637, p<0.01, two-ANOVA) (Fig. 4).
263 The maximum and minimum CH_4 concentrations were recorded in August and June,
264 respectively (Fig. 4). Across the sampling dates, CH_4 concentration increased with
265 depth (Fig. 4). CH_4 was supersaturated relative to the atmosphere across all depths
266 and all dates, with the mean saturation level between 2447 and 109394 %. Across all
267 dates, 47% of the samples were 24.0- to 100.0-fold oversaturated and 53% of the

samples were > 250.0-fold oversaturated.

3.3. Temporal variations in CO_2 and CH_4 fluxes

In the farming period, CO_2 flux at the water-air interface varied between −25.0±3.4 and 20.7±4.0 mg m^{-2} h^{-1}, with negative values representing CO_2 absorption (Fig. 5a). In the non-farming period, CO_2 flux across the sediment-air interface varied between −114.0±34.1 and 28.4±45.4 mg m^{-2} h^{-1} (Fig. 5a). Overall, the ponds were neutral in terms of CO_2 during the farming period, but were a CO_2 sink in the non-farming period.

Large temporal variation in CH_4 flux was also noted (Fig. 5b). During the farming period, CH_4 flux across the water-air interface varied between 1.2±1.2 and 127.1±15.1 mg m^{-2} h^{-1}. In general, CH_4 flux were higher and more variable in the middle of farming period (from July to September) (Fig. 5b). In the non-farming period, CH_4 flux across the sediment-air interface varied from 0.2±0.2 to 20.2±5.2 mg m^{-2} h^{-1} (Fig. 5b). The average CH_4 flux in the farming period (35.7±1.2 mg m^{-2} h^{-1}) was significantly higher than that in the non-farming period (4.8±0.3 mg m^{-2} h^{-1}) (F = 19.827, p = 0.009).

3.4. Ebullitive and diffusive fluxes

Our results from the floating chambers showed distinct nonlinear increases in CH_4 concentration during the sampling period. In addition, the total CH_4 flux measured with the floating chamber method (Fig. 5b) were 1.5-164 times larger than the diffusive flux calculated from the gas transfer coefficient model, and the difference between the two values represents ebullitive flux (Fig. 6). During the farming period,

290 the CH_4 diffusion flux varied from 0.2 to 4.2 mg m^{-2} h^{-1} (mean ± SE 1.8±0.3 mg m^{-2}
291 h^{-1}), while the mean CH_4 ebullition varied from 0.5 to 125.7 mg m^{-2} h^{-1} (mean ± SE
292 34.7±10.8 mg m^{-2} h^{-1}). Overall, ebullition contributed over 90% (range 5 - 98%) of
293 the total CH_4 flux.

294 *3.5. Influence of environmental variables*

295 Correlations between GHG fluxes and several environmental variables were
296 significant but weak, as indicated by correlation coefficients of 0.28 to 0.66 (Table 1
297 and Table S2; equivalent to r^2 of 0.05 to 0.44).

298 For the farming period, dissolved CO_2 in the water was correlated positively with
299 temperature ($p<0.01$, Table S2) and negatively with atmospheric pressure, water pH,
300 EC and DO ($p<0.05$ or $p<0.01$, Table S2). CH_4 in the water was correlated positively
301 with pH, DOC, TDN and TDP ($p<0.05$ or $p<0.01$, Table S2). CO_2 and CH_4 fluxes
302 were correlated positively with water temperature ($p<0.05$, Table 1) while negatively
303 with DO and pH (except CH_4) ($p<0.05$ or $p<0.01$, Table 1). Based on multiple
304 regression analysis, CO_2 flux was best explained by DO (explained 23% of the
305 variance), and CH_4 emission could be partly explained by water temperature and TDP
306 (explained 23% of the variance) (Table 2).

307 During the non-farming period, CO_2 and CH_4 fluxes showed positive correlation
308 with sediment TC, TN, and SWC (only CH_4) ($p<0.01$, Table 1).

309 **4. Discussion**

310 *4.1. Depth profiles of dissolved CO_2 and CH_4*

311 This study explored the high-resolution vertical profiles of the dissolved CO_2 and

312 CH_4 concentration in coastal aquaculture ponds. Vertical variations in dissolved CO_2
313 and CH_4 have been observed in deep-water systems such as lakes (e.g., Bastviken et
314 al., 2008; Gerardo-Nieto et al., 2017; Lambert and Sommer, 2007; Martinez-Cruz et
315 al., 2015), reservoirs (e.g., Gerardo-Nieto et al., 2017; Wang et al., 2011, 2015) and
316 the ocean (e.g., Gülzow et al., 2014; Sierra et al., 2017). Across most sampling dates,
317 CO_2 concentration in our ponds did not vary much vertically (variation coefficient
318 between 4.5 and 30.5 %), indicating a relatively well-mixed water column (Fig. 3).
319 The strongest vertical gradient was observed in August when the surface water
320 contained 2-fold less CO_2 than the bottom water, likely a result of higher respiration
321 in the sediment and photosynthetic CO_2 uptake at the surface.

322 In contrast to the CO_2 profiles, our data showed clearly increasing CH_4 with water
323 depth throughout much of the farming period (Fig. 4). The strongest vertical gradient
324 was in mid-August when CH_4 was negligible at the surface whereas the bottom water
325 contained >100 μmol CH_4 L^{-1}. The very distinct CH_4 profile is the likely result of
326 strong methanogenesis in the sediment and CH_4 loss (oxidation and emission) at the
327 water-air interface (Bastviken et al., 2004; Gerardo-Nieto et al., 2017). Bioturbation
328 by the shrimps on the sediment would further enhance CH_4 flux from the sediment.

329 *4.2. CO_2 and CH_4 fluxes in the farming period*

330 During the farming period, CO_2 flux across the water-air interface was very
331 variable, fluctuating between net emission and net absorption (Fig. 5a). Similar
332 patterns have been found in other nutrient-rich, high-productivity aquatic systems
333 (e.g., lake, reservoir) (Gerardo-Nieto et al., 2017; Gruca-Rokosz et al., 2017; Wang et

334 al., 2011, 2015; Xing et al., 2006; Yang et al., 2011). CO_2 flux is influenced by factors
335 such as respiration, photosynthesis and remineralization of organic matter (Abnizova
336 et al. 2012; Ding et al., 2013). In this study, net CO_2 flux was negatively correlated
337 with DO (Table 1), indicating the important role of algal photosynthesis in CO_2
338 draw-down in the initial (from June to mid-July) and final stages (from
339 mid-September to mid-November) of farming. Notably, CO_2 emission did not
340 decrease (Fig. 5a) in spite of high Chl-*a* concentrations in the middle farming stage
341 (between late June and early September) (Yang et al., 2020). This may be due to the
342 relatively high water temperature and extensive heterotrophic metabolism, which
343 could have caused respiration and remineralization of organics to dominate over
344 photosynthesis. This explanation is consistent with the positive relationships between
345 water temperature and CO_2 flux (Table 1).

346 Strong seasonality of CH_4 emission has been found in the aquatic ecosystems (e.g.,
347 Borges, et al., 2018; Natchimuthu et al., 2016; Sierra et al., 2017; Xiao et al., 2017).
348 Notably, CH_4 production and emission both increase with the rise in temperature
349 (Vizza et al., 2017; Yang et al., 2018a; Yvon-Durocher et al., 2014). In the summer
350 months of August and September, CH_4 emission reached maximum values (Fig. 5b).
351 Our statistical analysis also confirmed the significant correlation between air / water
352 temperature and CH_4 emission in the farming period (Table 1). However, the
353 fluctuating range of CH_4 fluxes was substantially larger than those observed in air /
354 water temperature. The phenomenon was likely caused by variations in CH_4 ebullition.
355 In the present study, the CH_4 ebullition varied from 0.5 to 125.7 mg m^{-2} h^{-1}, which

356 shown a striking variability over time. Ebullition is a combination of CH_4 production
357 being fast enough to form bubbles in the sediment and the physical release of these
358 bubbles. Temperature affect the CH_4 production rate directly, and thereby indirectly
359 affect the bubble release rate as sediment bubbles will grow and gain buoyancy faster
360 when warmer. Bubbles can also be triggered physically by turbulence or pressure
361 changes, and after each ebullition event there is a "bubble recharge" lag-phase before
362 ebullition can happen again. Such effects of physical triggers of more extensive
363 ebullition events can be more important for the high ebullition variability than
364 temperature.

365 *4.3. CO_2 and CH_4 fluxes in the non-farming period*

366 After harvesting, farmers drain the aquaculture ponds for routine maintenance. A
367 previous study has shown that shrimp ponds act as a CO_2 source, releasing 21.6-116.6
368 mg m^{-2} h^{-1} in the non-farming period (Yang et al., 2018b). The initial exposure of the
369 sediment to air after drainage may allow oxygen penetration into the sediment, which
370 then promotes the decomposition of organic matter (e.g., food pellets and biological
371 residues) and microbial respiration (Yang et al., 2018b). In contrast to the previous
372 study, which covered only December-January of the non-farming period, our data
373 show that after the initial CO_2 emission in the first two weeks after drainage, the
374 shrimp ponds turned into a strong CO_2 sink in the remaining months of the
375 non-farming period (Fig. 5a). Field observation found some pioneer herbaceous plants
376 in the ponds from late 2017, which might be responsible for the net CO_2 uptake.

377 CH_4 flux from the sediment increased initially after drainage but then decreased

quickly towards a stable and low emission over time (Fig. 5b). The trend and the magnitude of CH_4 flux in this study were similar to a previous report (range 0.1-28.3 mg m^{-2} h^{-1}) (Yang et al. 2018b). The initial increase in CH_4 emission after drainage could be due to degassing of the sediment. Similarly, Harrison et al. (2017) found that a reservoir drawdown of only 0.5 m can already stimulate CH_4 ebullition. There were also similar temporal patterns of CH_4 flux and sediment water content (SWC) (Figs. 2d and 5b) and a significantly positive correlation between them (Table 1). Therefore, the extended decrease in CH_4 flux in the non-farming period could be explained by the decrease in SWC, which would create a more aerobic condition that was less favourable for methanogenesis (Dinsmore et al., 2009; Yang et al., 2013a). In addition, evaporation during the non-farming period would increase the sediment salinity, which may also suppress CH_4 production through the effects of iron stress on extracellular enzymes and the competitive failure of methanogens versus sulfate-reducing bacteria in using carbon substrates (e.g., Hu et al., 2017; Poffenbarger et al., 2011; Sun et al., 2013; Vizza et al., 2017; Welti et al., 2017). Furthermore, the gradual decrease in sediment carbon content (TC; Fig. 2) means less substrate to support methane production over time (Table 1).

4.4. Contribution of ebullitive flux to CH_4 emission

The current estimates of CH_4 emission in aquatic ecosystems are still largely constrained by data scarcity on ebullitive fluxes (Bastviken et al., 2011; Tušeret al., 2017; Wu et al., 2019; Yang et al., 2019). In this study, the ebullitive CH_4 fluxes were estimated to contribute more than 90% to the total CH_4 emission in the farming period.

Similarly large contributions of ebullition are found in rivers (Wu et al., 2019), lakes (e.g., Bastviken et al., 2004; Chuang et al., 2017; Wik et al., 2013; Xiao et al., 2017) and reservoirs (Deemer et al., 2016; Deshmukh et al., 2016; Rodriguez and Casper, 2018). Notably, ebullition in the middle stage of farming (from August to September) accounted for ~ 90% of the total CH_4 emission (Fig. 6). Higher CH_4 ebullition at this stage could be caused by the larger loads of organic matter (e.g., aquatic feed) and higher water temperature, which would enhance CH_4 bubble formation in sediments and transportation from sediment to water surface (Wu et al., 2019; Zhu et al., 2016).

The magnitude of CH_4 ebullitive flux in our shrimp ponds was similar to that in a shallow peat lake on the eastern part of Tibetan Plateau, China (Zhu et al., 2016) and a reservoir in Ohio, USA (Beaulieu et al., 2018) (Table S3). However, the overall average of CH_4 ebullitive flux in our ponds was substantially larger than those observed in north Siberian thermokarst lakes (Walter et al., 2006), mid-boreal lake in Finland (Huttunen et al., 2001), shallow eutrophic lake in Eastern China (Xiao et al., 2017), and three subarctic lakes in northernmost Sweden (Wik et al., 2013), northern boreal beaver pond (Dove et al., 1999), a subtropical river in China (Wu et al., 2019), and rivers in the Amazon Basin (Sawakuchi et al., 2014) (Table S3). The larger CH_4 ebullition make the total emission per unit area from our aquculture ponds much larger compared with most other aquatic ecosystems (e.g. Bastviken et al., 2011; Yang and Flower, 2012).

4.5. Contribution of farming period to the annual GHG emission

Combining data from this study with previous measurement of CO_2 emission

422 (Yang et al., 2018b), the annual cumulative GHG fluxes from these aquaculture ponds
423 were ca. -77.6 g CO_2 g m^{-2} yr^{-1} and 154.3 g CH_4 g m^{-2} yr^{-1}. The sustained-flux global
424 warming potential (SGWP, for gas emissions) and sustained-flux global cooling
425 potential (SGCP, for gas uptake) models were applied to calculate the radiative
426 forcing of CO_2 and CH_4 fluxes from the ponds over a 100-year period (Neubauer and
427 Megonigal, 2015; Tangen et al., 2016). The annual cumulative CO_2-eq emission from
428 the shrimp ponds was 7.1×10^3 g CO_2-eq m^{-2} yr^{-1}, with ca. 99% in the form of CH_4
429 emission and ca. 90% occurring in the farming period. Increasing warming due to
430 climate change and environmental contamination could further exacerbate CH_4
431 production and emission from aquaculture ponds (Yang, 2014; Yang et al., 2013a),
432 and developing an effective management strategy to minimize GHG release,
433 particularly CH_4, in the farming period will be an important task for the aquatic food
434 producers.

435 *4.6. Limitations and future research*

436 Our research focused on GHG (CO_2 and CH_4) dynamics in Min River Estuary
437 over a one-year period. Our results highlight the importance of taking into account the
438 spatiotemporal variations in dissolved GHG concentrations and fluxes, and further
439 studies in multiple estuaries can provide more information for inter-estuary
440 comparison and extrapolation. We only did daytime sampling, whereas some
441 researchers have observed diurnal differences in GHG fluxes in aquatic ecosystems.
442 For example, some studies have shown a lower or even negative CO_2 emission in
443 daytime but higher emission at night (e.g., Del Giorgio et al., 1999; Erkkilä et al.,

2018; Natchimuthu et al., 2014; Xing et al., 2004), whereas CH_4 flux shows the opposite diurnal pattern (Hartmann et al., 2020; Sieczko et al., 2020). However, the reported diurnal differences are less than 3-fold and a diel correction factor of 0.7 was suggested to adjust daytime fluxes to 24-h fluxes (Sieczko et al. 2020). If this factor is valid also for aquaculture systems, it illustrates the diel bias in our data and that this bias does not change the main results as we observed an order-of-magnitude difference between the farming period and the non-farming period; hence, our measurements were sufficient to characterise the differences in GHG fluxes between these time periods and from the ponds on an annual basis. Nevertheless, future work may include nighttime measurements to fully resolve the diurnal variations. Significant spatial variations in CH_4 ebullition have been observed in other aquatic ecosystems (e.g., river, lake, and reservoir) (e.g., Wik et al., 2013; Wu et al., 2019). Future field sampling should consider more sites and higher measurement frequency to better quantify ebullitive fluxes. Further research into CH_4 production and consumption including the relevant microbial compositions and activities, such as methanotrophs, methanogens and sulfate-reducing bacteria, within the ponds will improve our understanding of the carbon cycle and inform more effective measures to mitigate carbon emission (Yang et al., 2013b).

5. Conclusions

The fast expansion of aquaculture operation world-wide raises legitimate concerns about the related GHG emissions (MacLeod et al., 2020). This study shows that subtropical earthen aquaculture ponds are a more intensive CH_4 emission source per

466 m^2 than most inland water bodies. However, there were also vast differences in CO_2
467 and CH_4 fluxes between the farming and non-farming periods; therefore, excluding
468 the non-farming period could lead to gross overestimation of GHG emissions from
469 aquaculture ponds. Ebullitive CH_4 flux in our shrimp ponds were substantially larger
470 than those in many other aquatic systems, and was the dominant emission pathway.
471 Overall, our results provide a more comprehensive picture of GHG fluxes over an
472 annual cycle including both farming and non-farming periods, and shed light on the
473 large contribution of CH_4 ebullition to the total CH_4 emission.

474 **Declaration of Competing Interest**

475 The authors declare that they have no known competing financial interests or
476 personal relationships that could have appeared to influence the work reported in this
477 paper.

478 **Acknowledgments**

479 This research was supported by the National Science Foundation of China
480 (41671088 and 41801070), Minjiang Scholar Programme, the Research Grants
481 Council of the Hong Kong Special Administrative Region, China (CUHK458913,
482 14302014, 14305515), the CUHK Direct Grant (SS15481), the European Research
483 Council (ERC; grant agreement No 725546), and the Swedish Research Councils VR
484 (2016-04829) and FORMAS (2018-01794). We also would like to thank Guanghui
485 Zhao, and Ling Li of the School of Geographical Sciences, Fujian Normal University
486 for their field assistance.

487 **References**

Åberg, J., Jansson, M., Jonsson, A., 2010. Importance of water temperature and thermal stratification dynamics for temporal variation of surface water CO_2 in a boreal lake. J. Geophys. Res. 115, G02024. https://doi.org/10.1029/2009JG001085

Abnizova, A., Siemens, J., Langer, M., Boike, J., 2012. Small ponds with major impact: the relevance of ponds and lakes in permafrost landscapes to carbon dioxide emissions. Glob. Biogeochem. Cycles 26: GB2041. https://doi.org/10.1029/2011GB004237

Balmer, M.B., Downing, J.A., 2011. Carbon dioxide concentrations in eutrophic lakes: undersaturation implies atmospheric uptake. Inland Waters 1, 125-132. https://doi.org/10.5268/IW-1.2.366

Bastviken, D., Cole, J. J, Pace, M. L, Tranvik, L., 2004. Methane emissions from lakes: Dependence of lake characteristics, two regional assessments, and a global estimate. Glob. Biogeochem. Cycle 18, GB4009. https://doi.org/10.1029/2004GB002238

Bastviken, D., Cole, J. J, Pace, M. L, Van de Bogert, M. C., 2008. Fates of methane from different lake habitats: Connecting whole-lake budgets and CH_4 emissions. J. Geophys. Res.-Biogeo. 113(G2). https://doi.org/10.1029/2007JG000608

Bastviken, D., Tranvik, L.J., Downing, J.A., Crill, P.M., Enrich-Prast, A., 2011. Freshwater methane emissions offset the continental carbon sink. Science 331, 50. https://doi.org/10.1126/science.1196808

Beaulieu, J.J., Balz, D.A., Birchfield, M.K., Harrison, J.A., Nietch, C.T., Platz, M.C., Squier, W.C., Waldo, S., Walker, J.T., White, K.M., 2018. Effects of an experimental water-level drawdown on methane emissions from a eutrophic reservoir. Ecosystems 21(4), 657-674. https://doi.org/10.1007/s10021-017-0176-2

Bergman, I., Klarqvist, M., Nilsson M., 2000. Seasonal variation in rates of methane production from peat of various botanical origins: effects of temperature and substrate quality. FEMS Microbiol. Ecol. 33, 181-189.

Bureau of Fisheries of the Ministry of Agriculture, 2019. China Fishery Statistics Yearbook. China Agriculture Press, Beijing (in Chinese).

Borges, A.V., Speeckaert, G., Champenois, W., Scranton, M.I., Gypens, N., 2018. Productivity and temperature as drivers of seasonal and spatial variations of dissolved methane in the Southern Bight of the North Sea. Ecosystems 21(4), 583-599. https://doi.org/10.1007/s10021-017-0171-7

519 Chen, Y., Dong, S.L., Wang, F., Gao, Q.F., Tian, X.L., 2016. Carbon dioxide and methane fluxes
520 from feeding and no-feeding mariculture ponds. Environ. Pollut. 212, 489-497.
521 https://doi.org/10.1016/j.envpol.2016.02.039
522 Chen, Y., Dong, S.L., Wang, Z.N., Wang, F., Gao, Q.F., Tian, X.L., Xiong, Y.H., 2015. Variations
523 in CO_2 fluxes from grass carp *Ctenopharyngodon idella* aquaculture polyculture ponds.
524 Aquacult. Environ. Interact. 8, 31-40. https://doi.org/10.3354/aei00149
525 Chuang, P.-C., Young, M.B., Dale, A.W., Miller, L.G., Herrera-Silveira, J.A., Paytan, A., 2017.
526 Methane fluxes from tropical coastal lagoons surrounded by mangroves, Yucatán, Mexico, J.
527 Geophys. Res. Biogeosci., 122(5), 1156-1174. https://doi.org/10.1002/2017JG003761
528 Cole, J.J., Caraco, N.F., 1998. Atmospheric exchange of carbon dioxide in a low-wind oligotrophic
529 lake measured by the addition of SF6. Limnol. Oceanogr. 43(4), 647-656.
530 https://doi.org/10.4319/lo.1998.43.4.0647
531 Cunada, C.L., Lesack, L.F.W., Tank, S.E.,2018. Seasonal dynamics of dissolved methane in lakes
532 of the Mackenzie Delta and the role of carbon substrate quality. J. Geophys. Res-Biogeo.
533 123(2), 591-609. https://doi.org/10.1002/2017JG004047
534 Deemer, B.R., Harrison, J. A., Li, S., Beaulieu, J.J., DelSontro, T., Barros, N., Bezerra-Neto, J.F.,
535 Powers, S.M., Santos, M.A. D., Vonk, J.A., 2016. Greenhouse gas emissions from reservoir
536 water surfaces: a new global synthesis. BioScience 66(11), 949-964.
537 https://doi.org/10.1093/biosci/biw117
538 Del Giorgio, P.A., Cole, J.J., Caraco, N., Peter, R.H., 1999. Linking planktonic biomass and
539 metabolism to net gas fluxes in northern temperate lakes. Ecology 80, 1422-1431.
540 https://doi.org/10.1890/0012-9658.
541 Deshmukh, C., Guérin, F., Labat, D., Pighini, S., Vongkhamsao, A., Guédant, P., Rode, W., Godon,
542 A., Chanudet, V., Descloux, S., Serça, D., 2016. Low methane (CH_4) emissions downstream
543 of a monomictic subtropical hydroelectric reservoir (Nam Theun 2, Lao PDR).
544 Biogeosciences, 13(6), 1919-1932. https://doi.org/10.5194/bg-13-1919-2016
545 Ding, W., Zhu, R.B., Ma, D.W., Xu, H., 2013. Summertime fluxes of N_2O, CH_4 and CO_2 from the
546 littoral zone of Lake Daming, East Antarctica: effects of environmental conditions. Antarct.
547 Sci. 25(6), 752-762. https://doi.org/10.1017/s0954102013000242

548 Dinsmore, K.J., Skiba, U.M., Billett, M.F., Rees, R.M., 2009. Effect of water table on greenhouse
549 gas emissions from peatland mesocosms. Plant Soil 318, 229-242.
550 https://doi.org/10.1007/s11104-008-9832-9
551 Dove, A., Roulet, N., Crill, P., Chanton, J., Bourbonniere, R., 1999. Methane dynamics of a
552 northern boreal beaver pond. Ecoscience 6, 577-586.
553 https://doi.org/10.1080/11956860.1999.11682548
554 Downing, J.A., 2010. Emerging global role of small lakes and ponds: little things mean a lot.
555 Limnetica 29, 9-24.
556 Drake, T.W., Raymond, P.A., Spencer, R.G., 2018. Terrestrial carbon inputs to inland waters: A
557 current synthesis of estimates and uncertainty. Limnol. Oceanogr. Lett. 3(3), 132-142.
558 https://doi.org/10.1002/lol2.10055
559 Einola, E., Rantakari, M., Kankaala, P., Kortelainen, P., Ojala, A., Pajunen, H., Mäkelä, S., Arvola,
560 L., 2011. Carbon pools and fluxes in a chain of five boreal lakes: a dry and wet year
561 comparison. J. Geophys. Res. Biogeosci. 116, G03009.
562 http://dx.doi.org/10.1029/2010JG001636
563 Erkkilä, K.M., Ojala, A., Bastviken, D., Biermann, T., Heiskanen, J.J., Lindroth, A., Peltola, O.,
564 Rantakari, M., Vesala, T., Mammarella, I., 2018. Methane and carbon dioxide fluxes over a
565 lake: comparison between eddy covariance, floating chambers and boundary layer method.
566 Biogeosciences15(2), 429-445. https://doi.org/10.5194/bg-15-429-2018
567 FAO, 2017. Fishery and aquaculture statistics (global aquaculture production 1950-2014).
568 FishStatJ. http://www.fao.org/fishery/statistics/software/fishstatj/en.
569 Gerardo-Nieto, O., Astorga-España, M.S., Mansilla, A., Thalasso, F., 2017. Initial report on
570 methane and carbon dioxide emission dynamics from sub-Antarctic freshwater ecosystems: a
571 seasonal study of a lake and a reservoir. Sci. Total Environ. 593, 144-154.
572 http://dx.doi.org/10.1016/j.scitotenv.2017.02.144
573 Gruca-Rokosz, R., Bartoszek, L., Koszelnik, P., 2017. The influence of environmental factors on
574 the carbon dioxide flux across the water-air interface of reservoirs in southeastern Poland. J.
575 Environ. Sci. 56, 290–299.
576 Gülzow, W., Gräwe, U., Kedzior, S., Schmale, O., Rehder, G., 2014. Seasonal variation of methane
577 in the water column of Arkona and Bornholm Basin, western Baltic Sea. J. Marine Syst. 139,
578 332-347. http://dx.doi.org/10.1016/j.jmarsys.2014.07.013.

579 Gudasz, C., Bastviken, D., Steger, K., Premke, K., Sobek, S., Tranvik, L.J., 2010.
580 Temperature-controlled organic carbon mineralization in lake sediments, Nature, 466(7305),
581 478-481. https://doi.org/10.1038/nature09186
582 Harrison, J.A., Deemer, B.R., Birchfield, M.K., O' Malley, M.T., 2017. Reservoir water-level
583 drawdowns accelerate and amplify methane emission. Environ. Sci. Technol. 51(3),
584 1267-1277. https://doi.org/10.1021/acs.est.6b03185
585 Hartmann, J.F., Günthel, M., Klintzsch, T., Kirillin, G., Grossart, H.P., Keppler, F.,
586 Isenbeck-Schröter, M., 2020. High spatiotemporal dynamics of methane production and
587 emission in oxic surface water. Environ. Sci. Technol. 54(3), 1451-1463.
588 https://doi.org/10.1021/acs.est.9b03182
589 Holgerson, M.A., 2015. Drivers of carbon dioxide and methane supersaturation in small,
590 temporary ponds. Biogeochemistry 124(1-3): 305-318.
591 https://doi.org/10.1007/s10533-015-0099-y
592 Holgerson, M.A., Raymond, P. A., 2016. Large contribution to inland water CO_2 and CH_4
593 emissions from very small ponds. Nat. Geosci. 9(3), 222-226.
594 https://doi.org/10.1038/NGEO2654
595 Hu, B.B., Wang, D.Q., Zhou, J., Meng, W.Q., Li, C.W., Sun, Z.B., Guo, X., Wang, Z.L., 2018.
596 Greenhouse gases emission from the sewage draining rivers. Sci. Total Environ. 612,
597 1454-1462. https://doi.org/10.1016/j.scitotenv.2017.08.055
598 Hu, M.J., Ren,H. C., Ren, P., Li, J.B., Wilson, B.J., Tong, C., 2017. Response of gaseous carbon
599 emissions to low-level salinity increase in tidal marsh ecosystem of the Min River estuary,
600 southeastern China. J. Environ. Sci. 52, 210-222. http://dx.doi.org/10.1016/j.jes.2016.05.009
601 Hu, Z., Lee, J.W., Chandran, K., Kim, S., Sharma, K., Khanal, S.K., 2014. Influence of
602 carbohydrate addition on nitrogen transformations and greenhouse gas emissions of intensive
603 aquaculture system. Sci. Total. Environ. 470, 193-200.
604 https://doi.org/10.1016/j.scitotenv.2013.09.050
605 Hu, Z.Q., Wu, S., Ji, C., Zou, J.W., Zhou, Q.S., Liu, S.W., 2016. A comparison of methane
606 emissions following rice paddies conversion to crab-fish farming wetlands in Southeast China.
607 Environ. Sci. Pollut. Res. 23 (2), 1505-1515. https://doi.org/10.1007/s11356-015-5383-9
608 Huttunen, J.T.J., Lappalainen, K.M.K., Saarijärvi, E.E., Väsänen, T.T., Martikainen, P.J.P., 2001. A
609 novel sediment gas sampler and a subsurface gas collector used for measurement of the

610 ebullition of methane and carbon dioxide from a eutrophied lake. Sci. Total Environ., 266(1-3),
611 153-158. https://doi.org/10.1016/S0048-9697(00)00749-X
612 Inglett, K.S., Inglett, P.W., Reddy, K.R., Osborne, T.Z., 2012. Temperature sensitivity of
613 greenhouse gas production in wetland soils of different vegetation. Biogeochemistry 108,
614 77-90.
615 Ivanov, M.V., Pimenov, N.V., Rusanov, I.I., Lein, A.Y., 2002. Microbial processes of the methane
616 cycle at the north-western shelf of the Black Sea. Estuar. Coast. Shelf Sci. 54(3), 589-599.
617 https://doi.org/10.1006/ecss.2000.0667
618 Jakobs, G., Holtermann, P., Berndmeyer, C., Rehder, G., Blumenberg, M., Jost, G., Schmale, O.,
619 2014. Seasonal and spatial methane dynamics in the water column of the central Baltic Sea
620 (Gotland Sea). Cont. Shelf Res. 91, 12 -25. https://doi.org/10.1016/j.csr.2014.07.005
621 Kortelainen, P., Rantakari, M., Huttunen, J.T., Mattsson, T., Alm, J., Juutinen, S., Larmola, T.,
622 Silvola, J., Martikainen, P.J., 2006. Sediment respiration and lake trophic state are important
623 predictors of large CO_2 evasion from small boreal lakes. Glob. Change Biol. 12,1554-1567.
624 https://doi.org/10.1111/j.1365-2486.2006.01167.x
625 Lambert, W., Sommer, U., 2007. Limnoecology. Second ed. Oxford, New York.
626 Lorke, A., Bodmer, P., Noss, C., Alshboul, Z., Koschorreck, M., Somlai-Haase, C., Bastviken, D.,
627 Flury, S., McGinnis, D.F., Maeck, A., Müller, D., Premke, K., 2015. Technical note: Drifting
628 versus anchored flux chambers for measuring greenhouse gas emissions from running waters.
629 Biogeosciences 12(23), 7013-7024. https://doi.org/10.5194/bg-12-7013-2015
630 MacLeod, M.J., Hasan, M.R., Robb, D.H., Mamun-Ur-Rashid, M., 2020. Quantifying greenhouse
631 gas emissions from global aquaculture. Sci. Rep. 10(1), 11679.
632 https://doi.org/10.1038/s41598-020-68231-8
633 Marotta, H., Pinho, L., Gudasz, C., Bastviken, D., Tranvik, L.J., Enrich-Prast, A., 2014.
634 Greenhouse gas production in low-latitude lake sediments responds strongly to warming, Nat.
635 Clim. Change 4(6), 467-470. https://doi.org/10.1038/nclimate2222
636 Martinez-Cruz, K., Sepulveda-Jauregui, A., Walter Anthony, K., Thalasso, F., 2015. Geographic
637 and seasonal variation of dissolved methane and aerobic methane oxidation in Alaskan lakes.
638 Biogeosciences 12(15), 4595-4606. https://doi.org/10.5194/bg-12-4595-2015
639 Meyers, P.A., 1997. Organic geochemical proxies of paleoceanographic, paleolimnologic, and
640 paleoclimatic processes. Org. Geochem. 27 (5-6), 213-250.

https://doi.org/10.1016/S0146-6380(97)00049-1

Moore, T.R., De Young, A., Bubier, J.L., Humphreys, E.R., Lafleur, P.M., Roulet, N.T., 2011. A multi-year record of methane flux at the Mer Bleue Bog, southern Canada. Ecosystems 14, 646-657.

Natchimuthu, S., Panneer Selvam, B., Bastviken, D., 2014. Influence of weather variables on methane and carbon dioxide flux from a shallow pond. Biogeochemistry 119, 403-413. https://doi.org/10.1007/s10533-014-9976-z

Natchimuthu, S., Sundgren, I., Gålfalk, M., Klemedtsson, L., Crill, P., Danielsson, Å., Bastviken, D., 2016. Spatio-temporal variability of lake CH_4 fluxes and its influence on annual whole lake emission estimates. Limnol. Oceanogr. 61(S1), S13-S26. https://doi.org/10.1002/lno.10222

Natchimuthu, S., Sundgren, I., Gålfalk, M., Klemedtsson, L., Bastviken, D., 2017. Spatiotemporal variability of lake pCO_2 and CO_2 fluxes in a hemiboreal catchment, J. Geophys. Res. Biogeosci. 122, 30-49. https://doi.org/10.1002/2016JG003449

Neubauer, S.C., Megonigal, J.P., 2015. Moving beyond global warming potentials to quantify the climatic role of ecosystems. Ecosystems 18, 1000-1013.

National Oceanic and Atmospheric (NOAA), 2020. Carbon cycle greenhouse gases: Trends in CH4. Available in: https://www.esrl.noaa.gov/gmd/ccgg/trends_ch4/

Olsson, L., Ye, S., Yu, X., Wei, M., Krauss, K.W., Brix, H., 2015. Factors influencing CO_2 and CH_4 emissions from coastal wetlands in the Liaohe Delta, Northeast China. Biogeosciences 12, 4965–4977.

Poffenbarger, H.J., Needelman, B.A., Megonigal, J.P., 2011. Salinity influence on methane emissions from tidal marshes. Wetlands 31, 831-842. https://doi.org/10.1007/s13157-011-0197-0

Raymond, P.A., Hartmann, J., Lauerwald, R., Sobek, S., McDonald, C., Hoover, M., Butman, D., Striegl, R., Mayorga, E., Humborg, C., Kortelainen, P., Durr, H., Meybeck, M., Ciais, P., Guth, P., 2013. Global carbon dioxide emissions from inland waters. Nature 503, 355-359.

Roehm, C.L., Prairie, Y.T., del Giorgio, P.A., 2009. The pCO_2 dynamics in lakes in the boreal region of northern Québec. Canada. Glob. Biogeochem. Cycle 23, GB3013. https://doi.org/10.1029/2008GB003297

671 Rodriguez, M., Casper, P., 2018. Greenhouse gas emissions from a semi-arid tropical reservoir in
672 northeastern Brazil. Reg. Environ. Change, 18, 1901-1912.
673 https://doi.org/10.1007/s10113-018-1289-7
674 Rubbo, M., Cole, J., Kiesecker, J., 2006. Terrestrial subsidies of organic carbon support net
675 ecosystem production in temporary forest ponds: evidence from an ecosystem experiment.
676 Ecosystems 9, 1170-1176. https://doi.org/10.1007/s10021-005-0009-6
677 Sawakuchi, H.O., Bastviken, D., Sawakuchi, A.O., Krusche, A.V., Ballester, M.V.R., Richey, J.E.,
678 2014. Methane emissions from amazonian rivers and their contribution to the global methane
679 budget. Global Chang. Biol. 20 (9), 2829-2840. https://doi.org/10.1111/gcb.12646
680 Segers, R., 1998. Methane production and methane consumption: a review of processes
681 underlying wetland methane fluxes. Biogeochemistry 41, 23-51.
682 https://doi.org/10.1023/A:1005929032764
683 Sieczko, A.K., Duc, N.T., Schenk, J., Pajala, G., Rudberg, D., Sawakuchi, H.O., Bastviken, D.,
684 2020. Diel variability of methane emissions from lakes. PNAS 117(35), 21488-21494.
685 http://dx.doi.org/10.1073/pnas.2006024117
686 Sierra, A., Jiménez-López, D., Ortega, T., Ponce, R., Bellanco, M.J., Sánchez-Leal, R.,
687 Gómez-Parra, A., Forja, J., 2017. Spatial and seasonal variability of CH_4 in the eastern Gulf
688 of Cadiz (SW Iberian Peninsula). Sci. Total Environ. 590, 695-707.
689 http://dx.doi.org/10.1016/j.scitotenv.2017.03.030
690 Song, C.C., Xu, X.F., Tian, H.Q., Wang, Y.Y., 2009. Ecosystem-atmosphere exchange of CH_4 and
691 N_2O and ecosystem respiration in wetlands in the Sanjiang Plain, Northeastern China. Glob.
692 Chang. Biol. 15, 692-705. http://dx.doi.org/10.1111/j.1365-2486.2008.01821.x
693 Sun, Z.G., Wang, L.L., Tian, H.Q., Jiang, H.H., Mou, X.J., Sun, W.L., 2013. Fluxes of nitrous
694 oxide and methane in different coastal *Suaeda salsa* marshes of the Yellow River estuary,
695 China. Chemosphere 90(2), 856-865. http://dx.doi.org/10.1016/j.chemosphere.2012.10.004
696 Tangen, B.A., Finocchiaro, R.G., Gleason, R.A., Dahl, C.F., 2016. Greenhouse gas fluxes of a
697 shallow lake in south-central North Dakota, USA. Wetlands 36, 779-787.
698 https://doi.org/10.1007/s13157-016-0782-3
699 Tong, C., Morris, J.T., Huang, J.F., Xu, H., Wan, S.A., 2018. Changes in pore-water chemistry and
700 methane emission following the invasion of *Spartina alterniflora* into an oliogohaline marsh.
701 Limnol. Oceanogr. 63(1), 384-396. https://doi.org/10.1002/lno.10637

Tranvik, L.J., Downing, J.A., Cotner, J.B., Loiselle, S.A., Striegle, R.G., Ballatore, T.J., Dillon, P., Finlay, K., Fortino, K., Knoll, L.B., Kortelainen, P.L., Kutser, T., Larsen, S., Laurion, I., Leech, D.M., McCallister, S.L., McKnight, D.M., Melack, J.M., Overholt, E., Porter, J.A., Prairie, Y., Renwick, W.H., Roland, F., Sherman, B.S., Schindler, D.W., Sobek, S., Tremblay, A., Vanni, M.J., Verschoor, A.M., von Wachenfeldt, E., Weyhenmeyera, G.A., 2009. Lakes and reservoirs as regulators of carbon cycling and climate. Limnol. Oceanogr. 54(6), 2298–2314. https://doi.org/10.4319/lo.2009.54.6_part_2.2298

Trolle, D., Staehr, P.A., Davidson, T.A., Bjerring, R., Lauridsen, T.L., Sondergaard, M., Jeppesen, E., 2012. Seasonal dynamics of CO_2 flux across the surface of shallow Temperate Lakes. Ecosystems 15, 336-347. https://doi.org/10.1007/s10021-011-9513-z

Verdegem, M.C.J., Bosma, R.H., 2009. Water withdrawal for brackish and inland aquaculture, and options to produce more fish in ponds with present water use. Water Policy 11 (Suppl 1), 52-68. https://doi.org/10.2166/wp.2009.003

Vizza, C., West, W.E., Jones, S.E., Hart, J.A., Lamberti, G.A., 2017. Regulators of coastal wetland methane production and responses to simulated global change. Biogeosciences 14, 431-446. https://doi.org/10.5194/bg-14-431-2017

Walter, K.M., Zimov, S.A., Chanton, J.P., Verbyla, D., Chapin, F.S., 2006. Methane bubbling from Siberian thaw lakes as a positive feedback to climate warming. Nature 443(7107), 71-75. https://doi.org/10.1038/nature05040

Wanninkhof, R., 1992. Relationship between wind speed and gas exchange over the ocean. J. Geophys. Res. 97, 7373-7382. https://doi.org/10.1029/92JC00188

Welti, N., Hayes, M., Lockington, D., 2017. Seasonal nitrous oxide and methane emissions across a subtropical estuarine salinity gradient. Biogeochemistry 132, 55-69. https://doi.org/10.1007/s10533-016-0287-4

West, W.E., Coloso, J.J., Jones, S.E., 2012. Effects of algal and terrestrial carbon on methane production rates and methanogen community structure in a temperate lake sediment. Freshwater Biol. 57(5), 949-955. https://doi.org/10.1111/j.1365-2427.2012.02755.x

Wik, M., Crill, P.M., Varner, R.K., Bastviken, D., 2013. Multiyear measurements of ebullitive methane flux from three subarctic lakes. J. Geophys. Res.-Biogeo. 118, 1307-1321. https://doi.org/10.1002/jgrg.20103

World Meteorological Organization, 2017. WMO Greenhouse Gas Bulletin No.13 (October 2017).

https://library.wmo.int/opac/doc_num.php?explnum_id=3084. pdf.

Wang, F. S., Cao, M., Wang, B. L., Fu, J. N., Luo, W. Y., Ma, J., 2015. Seasonal variation of CO_2 diffusion flux from a large subtropical reservoir in East China. Atmos. Environ. 103, 129-137. https://doi.org/10.1016/j.atmosenv.2014.12.042

Wang, F.S., Wang, B.L., Liu, C.Q., Wang, Y.C., Guan, J., Liu, X.L.,Yu, Y.X., 2011. Carbon dioxide emission from surface water in cascade reservoirs-river system on the Maotiao River, southwest of China. Atmos. Environ. 45, 3827-3834. https://doi.org/10.1016/j.atmosenv.2011.04.014

Wang, Q., Liu, H., Sui, J., 2018. Mariculture: Developments, present status and prospects. In: Gui, J.F., Tang, Q., Li, Z., Liu, J., De Silva, S.S. (Eds.), Aquaculture in China: Success Stories and Modern Trends. John Wiley & Sons Ltd, Hoboken, N.J., pp. 38-54.

Wu, S., Hu, Z.Q., Hu, T., Chen, J., Yu, K., Zou, J.W., Liu, S.W., 2018. Annual methane and nitrous oxide emissions from rice paddies and inland fish aquaculture wetlands in Southeast China. Atmos. Environ. 175, 135-144. https://doi.org/10.1016/j.atmosenv.2017.12.008

Wu, S., Li, S.Q., Zou, Z.H., Hu, T., Hu, Z.Q., Liu , S.W., Zou, J.W., 2019. High methane emissions largely attributed to ebullitive fluxes from a subtropical river draining a rice paddy watershed in China. Environ. Sci. Technol. 53, 349-3507. https://doi.org/10.1021/acs.est.8b05286

Xiao, Q.T., Zhang, M., Hu, Z.H., Gao, Y.Q., Hu, C., Liu, C., Liu, S.D., Zhang, Z., Zhao, J.Y., Xiao, W., Lee, X., 2017. Spatial variations of methane emission in a large shallow eutrophic lake in subtropical climate. J. Geophys. Res.- Biogeo. 122(7), 1597-1614. https://doi.org/10.1002/2017jg003805

Xing, Y.P., Xie, P., Yang, H., Ni, L.Y., Wang, Y.S., Tang, W.H., 2004. Diel variation of methane fluxes in summer in a eutrophic subtropical lake in China. Journal of Freshwater Ecology 19(4), 639-644. https://doi.org/10.1080/02705060.2004.9664745

Xing, Y.P., Xie, P., Yang, H., Ni, L.Y., Wang, Y.S., Rong, K., 2005. Methane and carbon dioxide fluxes from a shallow hypereutrophic subtropical Lake in China. Atmos. Environ. 39, 5532-5540. https://doi.org/10.1016/j.atmosenv.2005.06.010

Xing, Y.P., Xie, P., Yang, H., Wu, A.P., Ni, L.Y., 2006. The change of gaseous carbon fluxes following the switch of dominant producers from macrophytes to algae in a shallow

subtropical lake of China. Atmos. Environ. 40(40), 8034-8043. https://doi.org/10.1016/j.atmosenv.2006.05.033

Yang, H., 2014. China must continue the momentum of green law. Nature 509, 535-535. https://doi.org/10.1038/509535a

Yang, H., Andersen, T., Dörsch, P., Tominaga, K., Thrane, J.-E., Hessen, D.O., 2015a, Greenhouse gas metabolism in Nordic boreal lakes. Biogeochemistry 126, 211-225.

Yang, H., Flower, R.J., 2012. Potentially massive greenhouse-gas sources in proposed tropical dams. Front. Ecol. Environ.10(5), 234-235. https://doi.org/10.1890/12.WB.014

Yang, H., Flower, R.J., Thompson, J.R., 2013a. Sustaining China's water resources. Science 339(6116), 141-141.

Yang, H., Flower, R.J., Thompson, J.R., 2013b. China's new leaders offer green hope. Nature 493(7431), 163-163.

Yang, H., Xie, P., Ni, L., Flower, R.J., 2011. Underestimation of CH_4 emission from freshwater lakes in China. Environ. Sci. Technol. 45(10), 4203-4204. https://doi.org/10.1021/es2010336

Yang, J.S., Liu, J.S., Hu, X.J., Li, X.X., Wang, Y., Li, H.Y., 2013. Effect of water table level on CO_2, CH_4 and N_2O emissions in a freshwater marsh of Northeast China. Soil Biol. Biochem. 61, 52-60. https://doi.org/10.1016/j.soilbio.2013.02.009

Yang, P., He, Q.H., Huang, J.F., Tong, C., 2015b. Fluxes of greenhouse gases at two different aquaculture ponds in the coastal zone of southe astern China. Atmos. Environ. 115, 269-277. https://doi.org/10.1016/j.atmosenv.2015.05.067

Yang, P., Bastviken, D., Jin, B.S., Mou, X.J., Tong, C., 2017a. Effects of coastal marsh conversion to shrimp aquaculture ponds on CH_4 and N_2O emissions. Estuar. Coast. Shelf S. 199, 125-131. https://doi.org/10.1016/j.ecss.2017.09.023

Yang, P., Lai, D.Y.F., Jin, B., Bastviken, D., Tan, L.S., Tong, C., 2017b. Dynamics of dissolved nutrients in the aquaculture shrimp ponds of the Min River estuary, China: Concentrations, fluxes and environmental loads. Sci. Total Environ. 603-604, 256-267. http://dx.doi.org/10.1016/j.scitotenv.2017.06.074

Yang, P., Yang, H., Lai, D.Y.F., Guo, Q.Q., Zhang, Y.F., Tong, C., Xu, C.B., Li, X.F., 2020. Large contribution of non-aquaculture period fluxes to the annual N_2O emissions from aquaculture ponds in Southeast China. J. Hydrol. 582, 124550. https://doi.org/10.1016/j.jhydrol.2020.124550

794 Yang, P., Zhang, Y.F., Lai, D.Y.F., Tan, L.S., Jin, B.S., Tong, C., 2018a. Fluxes of carbon dioxide
795 and methane across the water-atmosphere interface of aquaculture shrimp ponds in two
796 subtropical estuaries: The effect of temperature, substrate, salinity and nitrate. Sci. Total
797 Environ. 635, 1025-1035. https://doi.org/10.1016/j.scitotenv.2018.04.102
798 Yang, P., Lai, D.Y.F., Huang, J.F., Tong, C., 2018b. Effect of drainage on CO_2, CH_4, and N_2O
799 fluxes from aquaculture ponds during winter in a subtropical estuary of China. J. Environ. Sci.
800 65, 72-82. https://doi.org/10.1016/j.jes.2017.03.024
801 Yang, P., Lai, D.Y.F., Huang, J.F., Zhang, L.H., Tong, C., 2018c. Temporal variations and
802 temperature sensitivity of ecosystem respiration in three brackish marsh communities in the
803 Min River Estuary, southeast China. Geoderma 327, 138-150.
804 https://doi.org/10.1016/j.geoderma.2018.05.005
805 Yang, P., Zhang, Y., Yang, H., Zhang, Y. F., Xu, J., Tan, L.S., Tong, C., Lai, D.Y.F., 2019. Large
806 fine-scale spatiotemporal variations of CH_4 diffusive fluxes from shrimp aquaculture ponds
807 affected by organic matter supply and aeration in Southeast China. J. Geophys. Res.-Biogeo.
808 https://doi.org/10.1029/2019JG005025
809 Yuan, J.J., Xiang, J., Liu, D.Y., Kang, H., He, T.H., Kim, S., Lin, Y.X., Freeman, C., Ding, W.X.,
810 2019. Rapid growth in greenhouse gas emissions from the adoption of industrial-scale
811 aquaculture. Nat. Clim. Change 9(4), 318-322. https://doi.org/10.1038/s41558-019-0425-9
812 Yuan, J.J., Liu, D.Y., Xiang, J., He, T.H., Kang, H., Ding, W.X., 2021. Methane and nitrous oxide
813 have separated production zones and distinct emission pathways in freshwater aquaculture
814 ponds. Water Res. 190, 116739. https://doi.org/10.1016/j.watres.2020.116739
815 Yvon-Durocher, G., Allen, A.P., Bastviken, D., Conrad, R., Gudasz, C., St-Pierre, A., ThanhDuc,
816 N., del Giorgio, P.A., 2014. Methane fluxes show consistent temperature dependence across
817 microbial to ecosystem scales. Nature 507, 488-491. https://doi.org/10.1038/nature13164
818 Zha, G.C., Zhou, C.Q., Huang, J.R., He, J.G., 2006. On the characteristics of Litopenaeus
819 vannamei body length and weight growth at low salinity environment. Journal of Fisheries of
820 China, 30(4), 489-494. (in Chinese)
821 Zhang, L., Wang, L., Yin, K.D., Lü, Y., Zhang, D.R., Yang, Y.Q., Huang, X.P., 2013. Pore water
822 nutrient characteristics and the fluxes across the sediment in the Pearl River estuary and
823 adjacent waters, China. Estuar. Coast Shelf Sci. 133, 182–192. https://
824 doi.org/10.1016/j.ecss.2013.08.028

825 Zhang, D.X., Tian, X.L., Dong, S,L., Chen, Y., Feng, J., He, R.P., Zhang, K., 2020. Carbon dioxide
826 fluxes from two typical mariculture polyculture systems in coastal China. Aquaculture 521,
827 735041. https://doi.org/10.1016/j.aquaculture.2020.735041
828 Zhu, D., Wu, Y., Chen, H., He, Y. X., Wu, N., 2016. Intense methane ebullition from open water
829 area of a shallow peatland lake on the eastern Tibetan Plateau. Sci. Total Environ. 542, 57-64.
830 https://doi.org/10.1016/j.scitotenv.2015.10.087

Figure

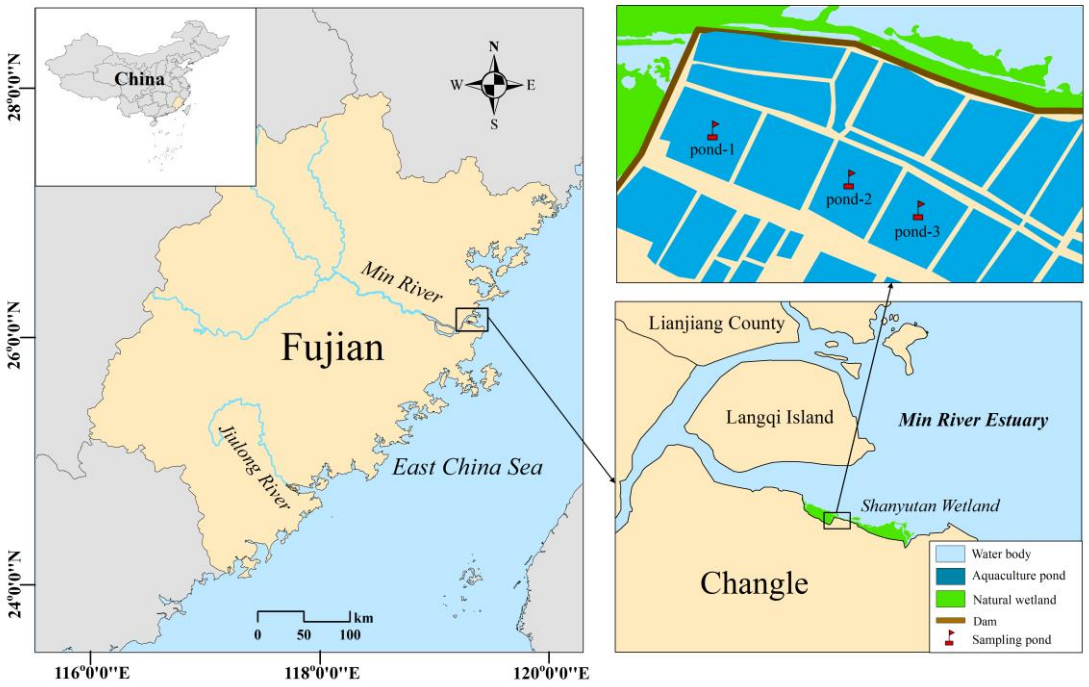

Fig. 1. Location of the researched aquaculture ponds in the Min River estuary, Fujian, Southeast China.

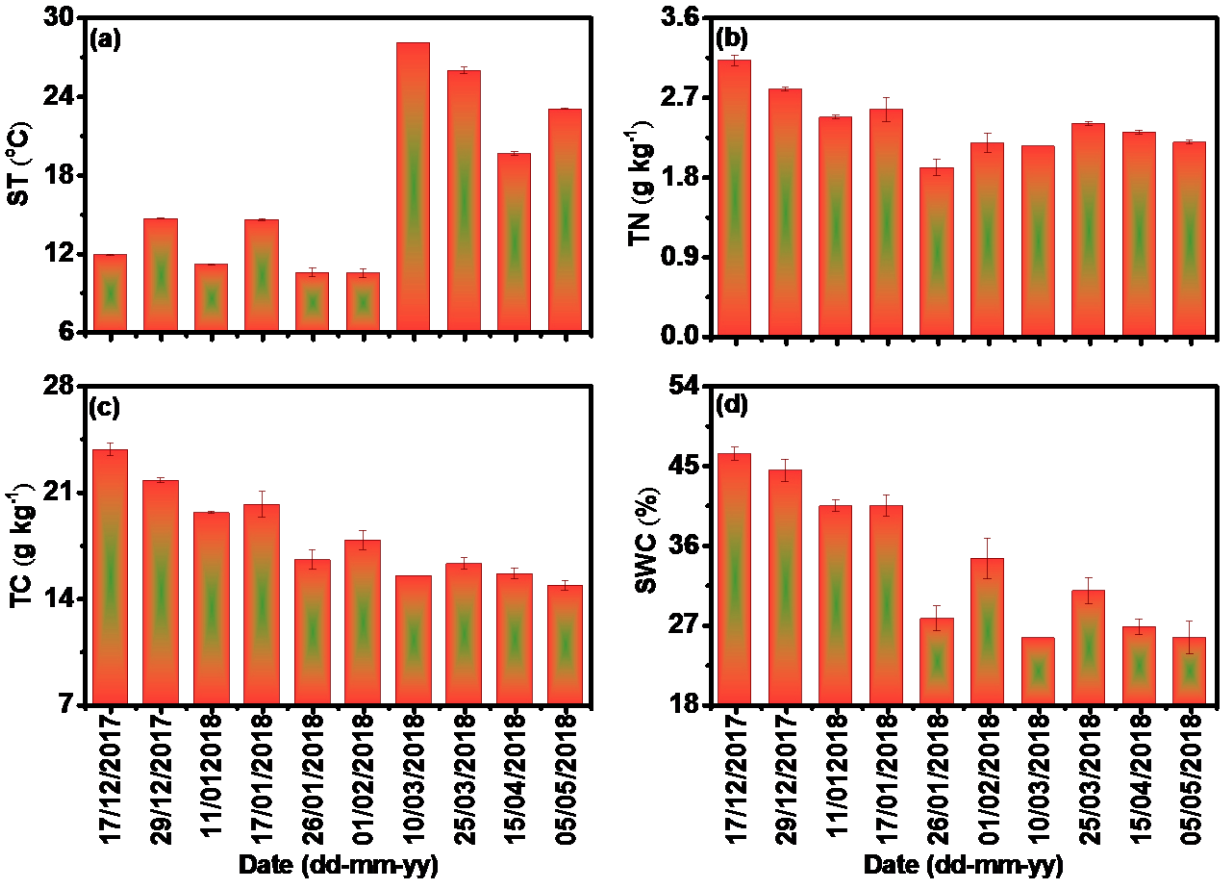

Fig. 2. Temporal variation in (a) sediment temperature at 15 cm depth, and (b) total carbon (TC) , (c) total nitrogen (TN), and (d) sediment water content (SWC) in surface sediments (0-15 cm) of aquaculture ponds in the Min River Estuary in the non-culture period. Bars are means±1 SE (n = 3 ponds).

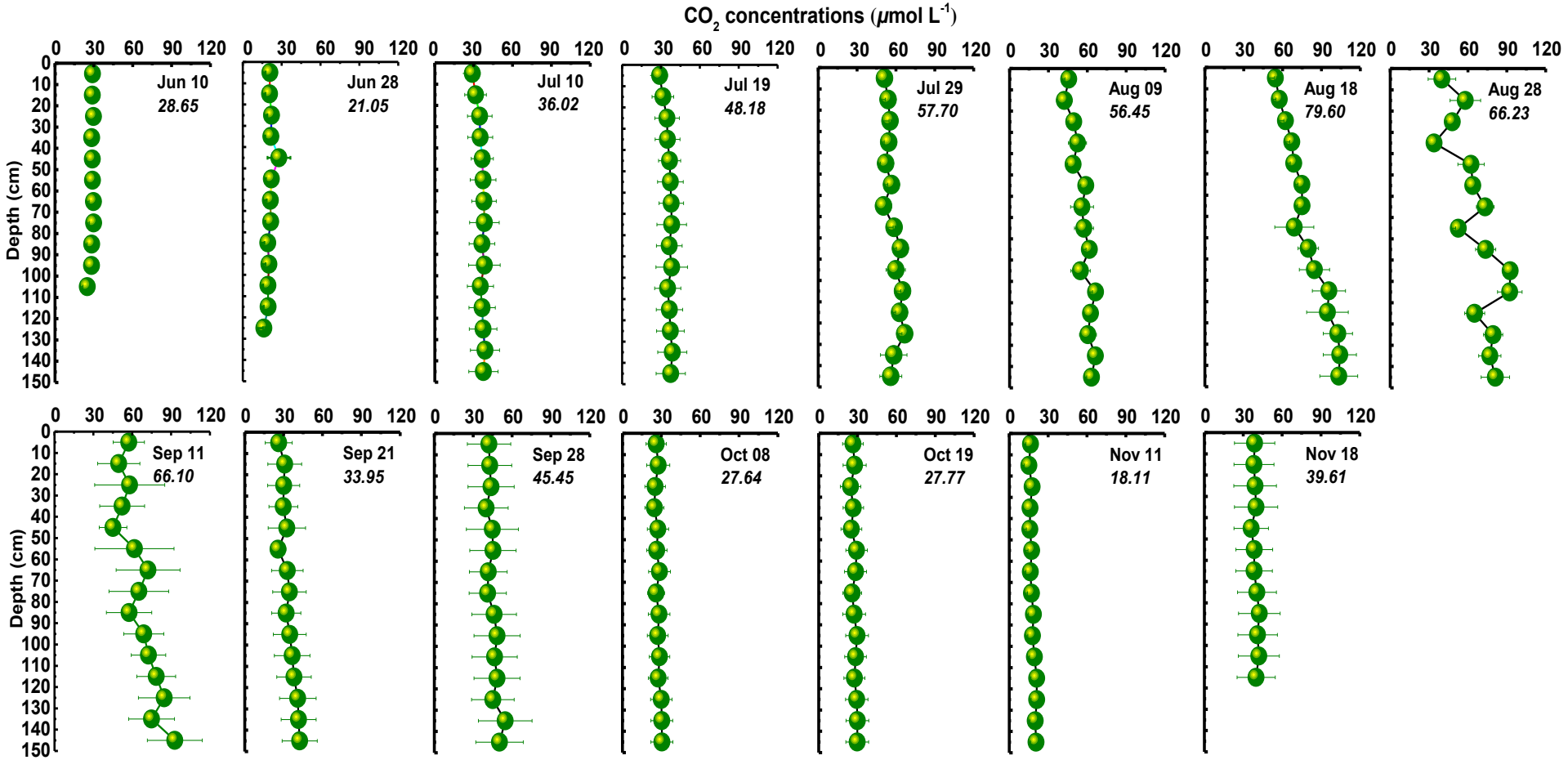

Fig. 3. The depth profiles of dissolved CO_2 concentration at mariculture ponds in the Min River Estuary in the culture period. *Error bars* represent standard error (n = 3 ponds). The *italics* numbers below the dates are the average concentrations from surface to bottom layer.

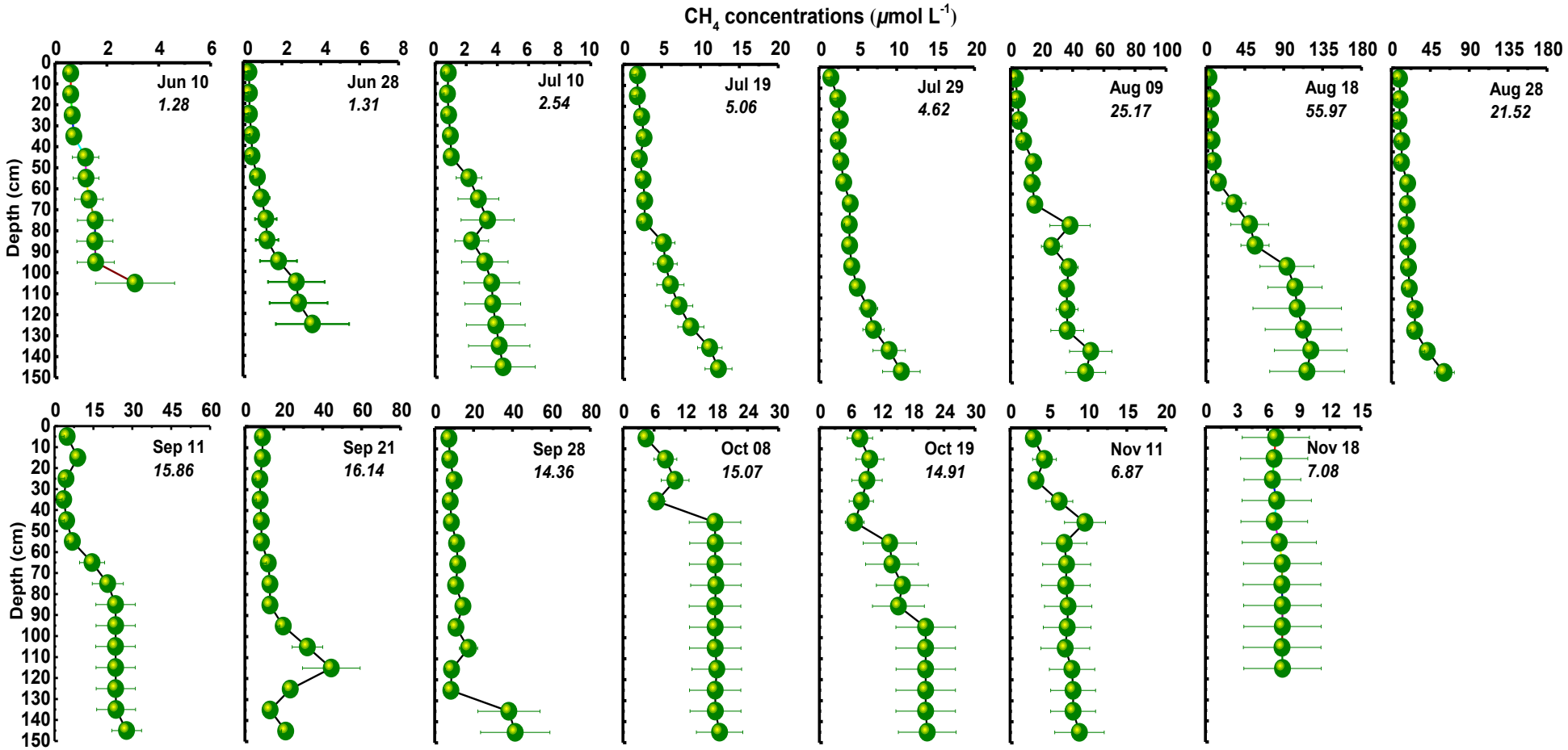

Fig. 4. The depth profiles of dissolved CH_4 concentration at mariculture ponds in the Min River Estuary in the culture period. *Error bars* represent standard error (n = 3 ponds). The *italics* numbers below the dates are the average concentrations from surface to bottom layer

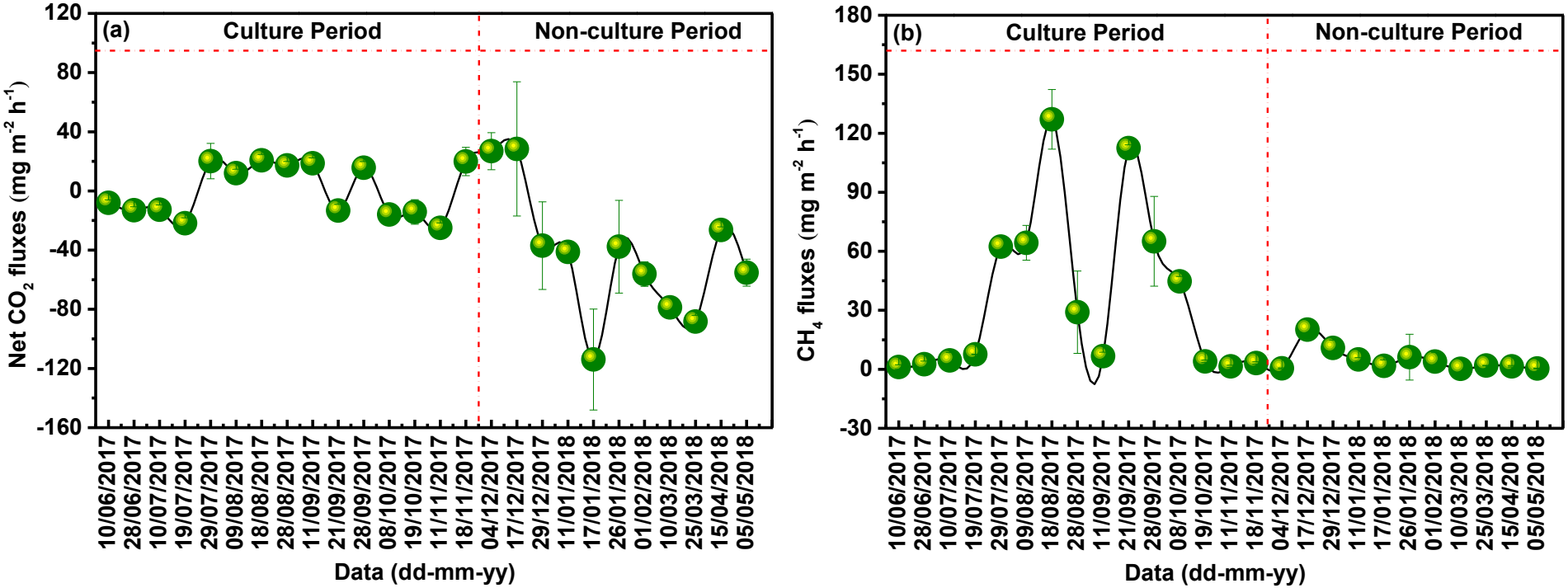

Fig. 5. CO_2 and CH_4 fluxes (mean ± SE) from the aquaculture ponds in the Min River Estuary in both aquaculture and non-aquaculture periods. The CH_4 fluxes represent the sum of diffusive flux and bubble flux. *Error bars* represent standard error (n = 3 ponds). The pond sediments were air-exposed during the non-culture period.

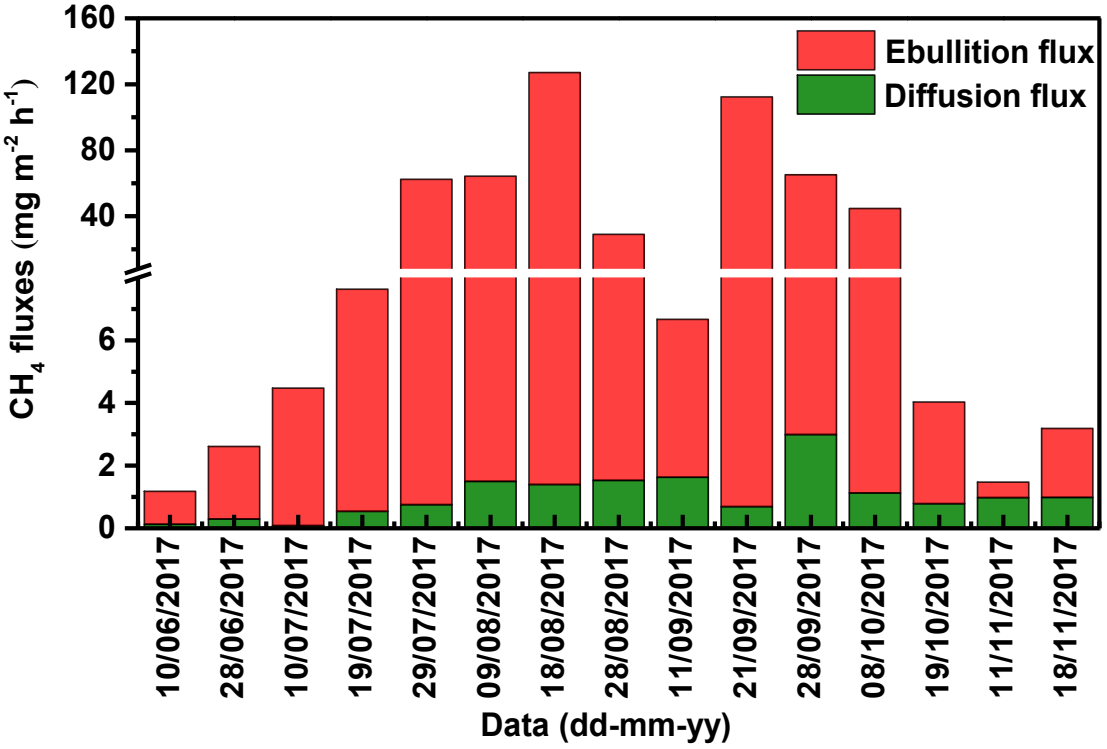

Fig. 6. CH_4 ebullitive fluxes *vs* diffusive fluxes from mariculture ponds in the culture period.

Table

Table 1

Pearson correlation coefficients for net CO_2 flux, CH_4 total flux and environmental variables at aquaculture ponds in the aquaculture period and the non-aquaculture period.

Environmental variables	Net CO_2 flux		CH_4 total flux	
	Aquaculture period[a]	Non-aquaculture period[b]	Aquaculture period[a]	Non-aquaculture period[b]
Meteorological factors				
Air temperature	NS		**0.323***	
Wind speed	NS		NS	
Atmospheric Pressure	**-0.295***		NS	
Physical and chemical properties of water				
Water temperature	**0.282***		**0.348***	
Conductivity (EC)	NS		NS	
pH	**-0.298***		NS	
Dissolved oxygen (DO)	**-0.480****		**-0.326***	
Dissolved organic carbon (DOC)	NS		NS	
Chlorophyll *a* (Chl *a*)	NS		NS	
Total dissolved nitrogen (TDN)	NS		NS	
Total dissolved phosphorus (TDP)	NS		NS	
Sediment properties				
Sediment temperature at 15 cm depth		**-0.334***		**-0.471***
Total carbon (TC)		**0.421***		**0.659****
Total nitrogen (TN)		**0.425****		**0.531****
Sediment water content (SWC)		NS		**0.543****

NS denotes "nonsignificant relationship." Bold numbers indicate the correlation coefficients for significant relationships. The symbols * and ** denote the significant correlations at $p < 0.05$ and 0.01, respectively. [a] $n = 45$ for environmental variables and GHGs fluxes at aquaculture ponds in the aquculture period; [b] $n = 33$ for environmental variables and GHGs fluxes at aquaculture ponds in the non-aquaculture period.

Table 2

Multiple regression equations between GHGs fluxes and environmental variables at the aquaculture ponds in Min River Estuary in the aquaculture period.

GHGs fluxes	**Regression equations**	***F***	R^2	***p***
CO_2 fluxes	$Y = 29.668 - 2.063x_{\text{Dissolved oxygen}}$	12.869	0.230	<0.001
CH_4 fluxes	$Y = -117.518 + 4.804x_{\text{Water temperature}} + 110.048x_{\text{TDP}}$	6.115	0.226	<0.005